Original Study

Prognostic Significance of ^{18}F-FDG PET/CT Metabolic Parameters and Tumor Galectin-1 Expression in Patients With Surgically Resected Lung Adenocarcinoma

Hongna Zheng,[1,2] Yan Cui,[1] Xuena Li,[1] Bulin Du,[1] Yaming Li[1]

Abstract

Galectin-1 (Gal-1) is a regulatory checkpoint that promotes immunosuppression and cancer development. We examined Gal-1 expression through immunohistochemistry and found that there was a significant positive correlation between Gal-1 expression and positron emission tomography/computed tomography (PET/CT) metabolic parameters in patients with surgically resected lung adenocarcinoma. Our results highlight PET/CT can predict Gal-1 expression and prognosis in lung adenocarcinoma.

Purpose: To study the prognostic significance of ^{18}F-fluorodeoxyglucose (^{18}F-FDG) positron emission tomography (PET)/computed tomography (CT) metabolic parameters and tumor galectin-1 (Gal-1) expression in patients surgically treated for lung adenocarcinoma. **Patients and Methods:** The medical records of 96 patients with primary lung adenocarcinoma who underwent surgery after ^{18}F-FDG PET/CT were retrospectively reviewed. The maximal standardized uptake value (SUV_{max}), metabolic tumor volume, and total lesion glycolysis of the primary tumor were measured through PET/CT imaging. The expression of tumor Gal-1, glucose transporter 1 (GLUT-1), and hexokinase II (HK-II) were examined through immunohistochemistry. **Results:** There were significant positive correlations between tumor Gal-1 and SUV_{max}, tumor Gal-1 and metabolic tumor volume, tumor Gal-1 and total lesion glycolysis, tumor Gal-1 and GLUT-1 expression, tumor Gal-1 and HK-II expression, and SUV_{max} and tumor GLUT-1 and HK-II expression ($P < .0001$ in all cases). SUV_{max} was the only independent predictor of tumor Gal-1 expression. On receiver operating characteristic analysis, the optimal cutoff value of SUV_{max} for predicting tumor Gal-1 expression was 5.1. Progression-free and overall survival were significantly shorter in patients with Gal-1−positive tumors than in those with Gal-1−negative tumors ($P \leq .001$). On multivariate analysis, advanced tumor stage ($P = .001$) and tumor Gal-1 expression ($P < .0001$) were independent prognostic indicators of poor progression-free survival, while advanced tumor stage ($P < .0001$) and SUV_{max} ($P = .024$) were independent prognostic indicators of poor overall survival. **Conclusion:** ^{18}F-FDG PET/CT has the potential to be used as a noninvasive imaging modality to assess tumor Gal-1 status and prognosis in lung adenocarcinoma.

Clinical Lung Cancer, Vol. 20, No. 6, 420-8 © 2019 Published by Elsevier Inc.

Keywords: ^{18}F-fluorodeoxyglucose, Immune biomarker, Lung cancer, Positron emission tomography, Prognosis

Introduction

Globally, non−small-cell lung cancer (NSCLC) is the leading cause of cancer-related death among men and women.[1] Lung adenocarcinoma is the most common histologic subtype of NSCLC, accounting for more than 50% of cases.[2] Despite significant advances in surgery, chemotherapy, and molecular targeted therapy, the 5-year overall survival (OS) rate in patients with NSCLC remains poor.[3]

Most recently, immunotherapy is giving new hope to patients with advanced lung adenocarcinoma. In particular, the use of

[1]Department of Nuclear Medicine, The First Hospital of China Medical University, Shenyang, China
[2]Department of Nuclear Medicine, The First Hospital of Dalian Medical University, Dalian, China

Submitted: Feb 12, 2019; Revised: Apr 2, 2019; Accepted: Apr 10, 2019; Epub: May 17, 2019

Address for correspondence: Yaming Li, MD, Department of Nuclear Medicine, The First Hospital of China Medical University, North Nanjing Street 155, Shenyang 110001, China
E-mail contact: ymli2001@163.com

1525-7304/$ - see frontmatter © 2019 Published by Elsevier Inc.
https://doi.org/10.1016/j.cllc.2019.04.002

immune checkpoint inhibitors has resulted in a remarkable paradigm shift in the treatment options that are available for NSCLC and are yielding promising clinical outcomes.[4] However, not all patients have disease that responds to immune checkpoint inhibitors, as tumors may develop compensatory pathways to generate resistance to these drugs.[5] Consequently, there remains an unmet clinical need to identify new immune biomarkers and therapeutic targets in NSCLC.

Galectins have emerged as regulatory checkpoints that promote immunosuppression and cancer development.[6] Galectin-1 (Gal-1) is the prototype member of the galectin superfamily. Gal-1 is characterized by its high affinity binding to β-galactosides through a highly conserved carbohydrate recognition domain.[7] Gal-1 activates the HIF/mTOR, Notch1/Jagged2, NF-κB, and MAPK pathways,[8-11] and is involved in tumor cell proliferation, adhesion, migration, and aggregation as well as angiogenesis and immune evasion.[12-17] Gal-1 is overexpressed in many cancer types, including lung cancer, and has been associated with poor survival.[18-21] Therefore, tumor Gal-1 status may be a potential predictive biomarker of poor prognosis. Immunohistochemistry is the reference standard in Gal-1 testing. However, the availability of a sufficient quality and quantity of tissue for Gal-1 testing often remains a challenge, and noninvasive imaging modalities that predict Gal-1 status could be beneficial.

^{18}F-fluorodeoxyglucose (^{18}F-FDG) positron emission tomography (PET)/computed tomography (CT) is a noninvasive imaging tool that is frequently used in the management of lung cancer.[22] FDG uptake reflects glucose metabolism in malignant cells. A previous study showed that Gal-1 expression was linked to upregulated glucose transport and uptake in mouse embryonic stem cells.[23] Furthermore, Gal-1 has been shown to trigger the activation of glycolysis-related enzymes and promote lactate production in colon cancer cells.[24] Currently, the relationship between FDG uptake and Gal-1 expression in lung adenocarcinoma is unknown. Therefore, the aim of this study was to investigate the correlation and prognostic value of PET/CT metabolic parameters and tumor Gal-1 expression in patients who underwent surgery for lung adenocarcinoma.

Patients and Methods

Patients

The medical records of 96 patients with primary lung adenocarcinoma who underwent surgery after ^{18}F-FDG PET/CT at the First Affiliated Hospital of Dalian Medical University between May 2010 and October 2015 were retrospectively reviewed. The inclusion criteria were as follows: histopathologic confirmation of primary lung adenocarcinoma, and ^{18}F-FDG PET/CT scan performed within 30 days before surgery. The exclusion criteria were as follows: neoadjuvant treatment was provided before surgery, and the patient had a history of another malignancy. The clinicopathologic characteristics of each patient, including age, sex, smoking status, tumor differentiation, and tumor, node, metastasis classification system stage assessed at surgical resection (according to 7th edition of the American Joint Committee on Cancer lung cancer staging system[25]), were recorded. This study was approved by the ethics committee of the First Affiliated Hospital of Dalian Medical University, and informed consent was waived in this retrospective study.

^{18}F-FDG PET/CT Imaging Procedures

PET/CT was performed using a Biograph True Point PET/CT scanner (Siemens Medical Systems). Patients fasted for 6 to 8 hours to obtain a blood glucose level ≤ 6.6 mmol/L before intravenous injection of 0.15 mCi/kg FDG. Approximately 60 minutes after FDG administration, PET/CT scans were acquired from the base of the skull to the proximal thigh. Immediately after CT scanning (tube voltage, 120 kV; CARE Dose, tube current, 60−80 mA; with shallow breathing), PET imaging in 3-dimensional mode was performed using an acquisition time of 1.5 minutes per bed position. PET images were reconstructed using ordered subset expectation maximization with attenuation correction. ^{18}FDG PET/CT images were reviewed at a standard workstation (MMWP; Siemens) by 2 physicians with experience in nuclear medicine. The maximal standardized uptake value (SUV_{max}) of the primary tumor was measured using a region of interest that was manually placed over the lesion. The region of interest was drawn on the basis of the corresponding CT image for lesions with inconclusive PET findings. Metabolic tumor volume (MTV) was defined using a predetermined SUV_{max} threshold of 2.5. Total lesion glycolysis (TLG) was calculated as: mean SUV × MTV.

Immunohistochemistry

Immunohistochemistry was performed on 4 μm thick tissue sections that were cut from paraffin-embedded lung adenocarcinoma specimens. The primary antibodies that were used included anti−Gal-1 (dilution 1:200; Abcam), anti−glucose transporter 1 (GLUT-1; dilution 1:500; Abcam), and anti−hexokinase II (HK-II; dilution 1:200; Abcam). All sections were semiquantitatively evaluated by 2 experienced pathologists in a blinded manner. Staining intensity was categorized as 0 (negative), 1 (weak), 2 (moderate), or 3 (strong), and the percentage of positive cells was categorized as 0 (0), 1+ (≤ 10%), 2+ (11-50%), 3+ (51-80%), or 4+ (> 80%).

The immunohistochemistry scores for each protein were calculated by multiplying the staining intensity by the percentage of positive cells.[26] The final score was classified as negative (0−4) or positive (5−12).

Statistical Analysis

Statistical analyses were performed by SPSS 22.0 software (IBM, Armonk, NY). The chi-square and Fisher exact test were used to analyze the relationships between the categorical variables. The Mann-Whitney *U* test or *t* test was used to analyze the associations between continuous variables, when appropriate. Spearman correlation analysis was used to evaluate correlations among SUV_{max} and tumor Gal-1, GLUT-1, and HK-II expression. Logistic regression analysis was used to identify independent predictors of tumor Gal-1 expression. A receiver operating characteristic (ROC) curve was constructed to obtain the optimal cutoff value of SUV_{max} for predicting the tumor Gal-1 expression.

Progression-free survival (PFS) was defined as the time from the date of surgery to tumor recurrence or cancer-related death. OS was defined as the time from the date of surgery to all-cause death or last follow-up. PFS and OS were calculated by the Kaplan-Meier method, and the log-rank test was used for comparisons. Multivariate survival analysis was performed using the Cox proportional hazards model. $P < .05$ was considered statistically significant.

Figure 1 Representative Images of ^{18}F-FDG PET/CT and Immunohistochemistry of Gal-1, GLUT-1, and HK-II. (A) PET. (B) CT. (C) PET/CT. (D) Gal-1. (E) GLUT-1. (F) HK-II. Original Magnification, ×200

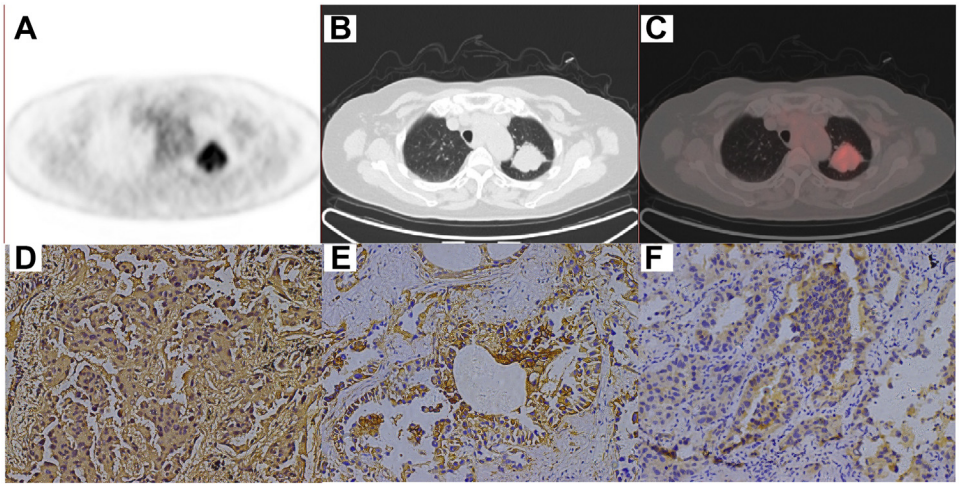

Abbreviations: CT = computed tomography; ^{18}F-FDG = ^{18}F-fludeoxyglucose; Gal-1 = galectin-1; GLUT-1 = glucose transporter 1; HK-II = hexokinase II; PET = positron emission tomography.

Results

Patient Characteristics

A total of 96 patients with primary lung adenocarcinoma who underwent ^{18}F-FDG PET/CT in the 30-day period before surgery were included in this study. Representative PET/CT images are displayed in Figure 1.

Among the included patients, there were 55 women and 41 men. The mean age of patients was 64.6 years (range, 41−86 years). The

Table 1 Associations Between Tumor Gal-1 Expression and Clinical Characteristics in Primary Lung Adenocarcinoma

Characteristic	Tumor Gal-1 Expression		Total	*P*
	Negative (N = 54)	Positive (N = 42)		
Age (y), mean ± SD	65.1 ± 9.2	63.9 ± 9.0	64.6 ± 9.1	.519
Sex				.979
Male	23 (56.1)	18 (43.9)	41 (42.3)	
Female	31 (56.4)	24 (43.6)	55 (57.3)	
Smoking History				.260
Smoker	20 (64.5)	11 (35.5)	31 (32.3)	
Nonsmoker	34 (52.3)	31 (47.7)	65 (67.7)	
Tumor Differentiation				<.0001
Well	34 (85.0)	6 (15.0)	40 (41.7)	
Moderate/poor	20 (35.7)	36 (64.3)	56 (58.3)	
Tumor size (cm), median (range)	2.0 (0.4-5.2)	2.5 (0.9-6.5)	2.2 (0.4-6.5)	.013
Lymph Node Metastasis				<.0001
N_0	53 (73.6)	19 (26.4)	72 (75.0)	
$N_{\geq 1}$	1 (4.2)	23 (95.8)	24 (25.0)	
TNM Stage				<.0001
I + II	52 (67.5)	25 (32.5)	77 (80.2)	
III + IV	2 (10.5)	17 (89.5)	19 (19.8)	
SUV_{max}, median (range)	2.6 (0.7-11.4)	10.8 (0.9-23.3)	5.0 (0.7-23.3)	<.0001
MTV, median (range)	0.1 (0.0-14.0)	7.1 (0.0-93.2)	2.0 (0.0-93.2)	<.0001
TLG, median (range)	0.1 (0.0-70.6)	33.5 (0.0-480.0)	7.2 (0.0-478.9)	<.0001

Data are presented as n (%) unless otherwise indicated.
Abbreviations: Gal-1 = galectin-1; MTV = metabolic tumor volume; SD = standard deviation; SUV_{max} = standardized maximum uptake value; TLG = total lesion glycolysis; TNM = tumor, node, metastasis classification system.

Figure 2 Scatter Plots Evaluating Associations Among SUV_{max} and Tumor Gal-1, GLUT-1, and HK-II Expression. (A) SUV_{max} and Tumor Gal-1. (B) Tumor GLUT-1 and Gal-1. (C) Tumor HK-II and Gal-1. (D) SUV_{max} and Tumor GLUT-1. (E) SUV_{max} and Tumor HK-II

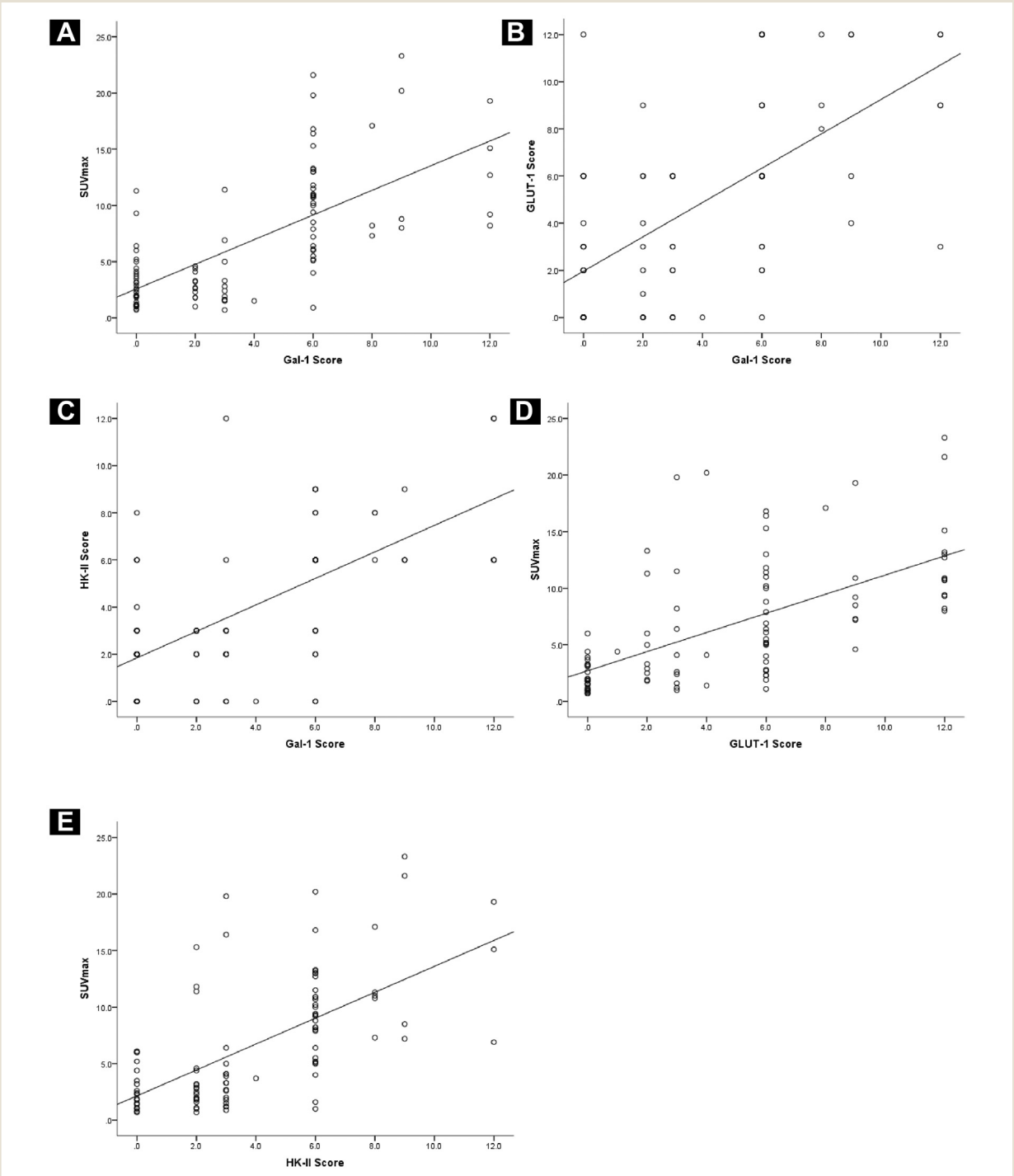

Abbreviations: Gal-1 = galectin-1; GLUT-1 = glucose transporter 1; HK-II = hexokinase II; SUV_{max} = maximal standardized uptake value.

median tumor size was 2.2 cm (range, 0.4–6.5 cm). Sixty-four (66.7%), 13 (13.5%), 14 (14.6%), and 5 (5.2%) patients had stage I, stage II, stage III, and stage IV disease, respectively. Lymph node metastasis was detected in 24 patients. Of these, 9 had N1 disease, 14 had N2 disease, and 1 had N3 disease. The median SUV_{max}, MTV, and TLG of the primary tumor were 5.0 (range, 0.7–23.3), 2.0 (range, 0.0–93.2), and 7.2 (range, 0–478.9), respectively (Table 1).

Table 2 Univariate and Multivariate Analysis of Clinical Characteristics Associated With Tumor Gal-1 Expression in Primary Lung Adenocarcinoma

	Univariate Analysis		Multivariate Analysis	
Characteristic	**OR (95% CI)**	***P***	**OR (95% CI)**	***P***
Age	0.985 (0.942-1.030)	.515		
Sex		.979		
Male	Reference			
Female	0.989 (0.438-2.235)			
Smoking History		.261		
Smoker	0.603 (0.250-1.457)			
Nonsmoker	Reference			
Tumor Differentiation		<.0001		.400
Well	Reference			
Moderate/poor	10.200 (3.657-28.448)			
Tumor size	1.653 (1.111-2.460)	.013		.360
Lymph Node Metastasis		<.0001		.280
N_0	Reference			
$N_{\geq 1}$	64.158 (8.099-508.224)			
TNM Stage		<.0001		.382
I + II	Reference			
III + IV	17.680 (3.787-82.540)			
SUV_{max}	1.839 (1.456-2.323)	<.0001	1.581 (1.149-2.176)	.005
MTV	1.426 (1.186-1.716)	<.0001		.251
TLG	1.092 (1.040-1.147)	<.0001		.315

Abbreviations: CI = confidence interval; Gal-1 = galectin-1; MTV = metabolic tumor volume; OR = odds ratio; SUV_{max} = standardized maximum uptake value; TLG = total lesion glycolysis; TNM = tumor, node, metastasis classification system.

Associations Between Clinical Characteristics and Tumor Gal-1 Expression

The expression of Gal-1 protein was primarily observed in the cytoplasm or on the membrane of lung adenocarcinoma cells (Figure 1). Immunohistochemistry scores were used to stratify patients as Gal-1 positive (n = 42) or negative (n = 54). Gal-1 positivity occurred more frequently in patients with lymph node metastasis, advanced stage tumors, and moderately or poorly differentiated carcinoma ($P < .0001$ in all cases; Table 1). The tumor size was larger ($P = .013$) and SUV_{max}, MTV, and TLG were significantly higher in the Gal-1−positive patients than in Gal-1−negative patients ($P < .0001$ in all cases). There were no significant differences in age, sex, or smoking history between the Gal-1−positive and Gal-1−negative patients (Table 1).

Association Between SUV_{max} and Tumor Gal-1 Expression

There was a significant positive correlation between SUV_{max} and the immunohistochemistry score for Gal-1 (rho = 0.690; $P < .0001$; Figure 2). On univariate analysis, the tumor size, nodal involvement, tumor stage, tumor differentiation, SUV_{max}, MTV, and TLG were significantly associated with tumor Gal-1 expression.

On multivariate regression analysis, SUV_{max} was the only independent predictor of tumor Gal-1 expression (Table 2).

ROC curve analysis was used to evaluate the ability of SUV_{max} to discriminate tumor Gal-1 expression in primary lung adenocarcinoma. The area under the curve was 0.937 (95% confidence interval, 0.882−0.992) and the P value was < .0001, suggesting that SUV_{max} has the ability to predict tumor Gal-1 expression. The optimal cutoff value of SUV_{max} for predicting tumor Gal-1 expression was 5.1, at which point SUV_{max} predicted tumor Gal-1 expression with 95.2% sensitivity and 87.0% specificity (Figure 3).

Associations Among SUV_{max} and Tumor Gal-1, GLUT-1, and HK-II Expression

The expression of the GLUT-1 and HK-II proteins were primarily localized on the membrane of lung adenocarcinoma cells (Figure 1). There were significant positive correlations between the immunohistochemistry scores for Gal-1 and GLUT-1 (rho = 0.647; $P < .0001$) and Gal-1 and HK-II (rho = 0.644; $P < .0001$). There were significant positive correlations between SUV_{max} and immunohistochemistry score for GLUT-1 (rho = 0.680; $P < .0001$) or HK-II (rho = 0.642; $P < .0001$; Figure 2).

Tumor Gal-1 Expression and Prognosis

The median follow-up time was 58.5 months (range, 11−105 months). During this period, 35 patients had recurrent disease, and 20 patients died from cancer-related causes. The median PFS in Gal-1−positive patients was 16.0 months (range, 1−62 months), and the median PFS in Gal-1−negative patients was 61.0 months (range, 36−105). The median OS in Gal-1−positive patients was 25.5 months (range, 1−62 months), and the median OS in Gal-1−negative patients was 62.0 months (range, 36−105 months).

Figure 3 ROC Curve Analysis Evaluating Ability of SUV_{max} to Discriminate Gal-1 Expression in Primary Lung Adenocarcinoma. AUC Was 0.937 (95% Confidence Interval, 0.882-0.992; $P < .001$). When Cutoff Value of SUV_{max} Was 5.1, SUV_{max} Predicted Tumor Gal-1 Expression With 95.2% Sensitivity and 87.0% Specificity

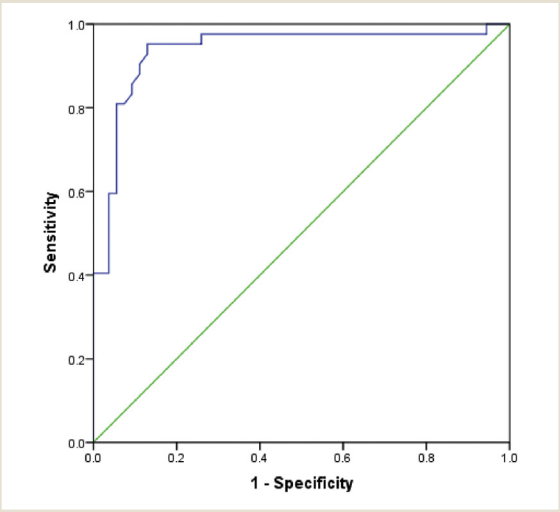

Abbreviations: AUC = area under the plasma concentration versus time curve; Gal-1 = galectin-1; ROC = receiver operating characteristic; SUV_{max} = maximal standardized uptake value.

The PFS and OS were significantly shorter in the Gal-1−positive patients than in the Gal-1−negative patients ($P \leq .001$; Figure 4).

On univariate analysis, nodal involvement, tumor stage, tumor differentiation, tumor Gal-1 expression, SUV_{max}, MTV, and TLG were significantly associated with PFS, while sex, nodal involvement, tumor stage, tumor Gal-1 expression, SUV_{max}, MTV, and TLG were significantly associated with OS. On multivariate analysis, advanced tumor stage ($P = .001$) and tumor Gal-1 expression ($P < .0001$) were independent prognostic indicators of poor PFS, while advanced tumor stage ($P < .0001$) and SUV_{max} ($P = .024$) were independent prognostic indicators of poor OS (Table 3).

Discussion

To our knowledge, this is the first study to demonstrate that ^{18}F-FDG PET/CT has potential as a noninvasive imaging modality in the assessment of tumor Gal-1 expression, which is a biomarker of poor survival in many cancers.[18-21] This study revealed that tumor Gal-1 expression was positively associated with glucose metabolism, evaluated by FDG PET, in primary lung adenocarcinoma cells. SUV_{max}, MTV, and TLG were significantly higher in Gal-1−positive patients than in Gal-1−negative patients, and SUV_{max} was the only independent predictor of tumor Gal-1 expression. ROC analysis identified an $SUV_{max} > 5.1$ as a significant predictor of tumor Gal-1 expression in primary lung adenocarcinoma. Immunohistochemistry is the reference standard in Gal-1 testing. However, obtaining sufficient quality and quantity of tissue for Gal-1 testing is often challenging. This study shows that ^{18}F-FDG PET/CT may be used to select patients who will gain the most benefit from

Figure 4 Kaplan-Meier Survival Curves for (A) PFS and (B) OS In Patients With Lung Adenocarcinoma

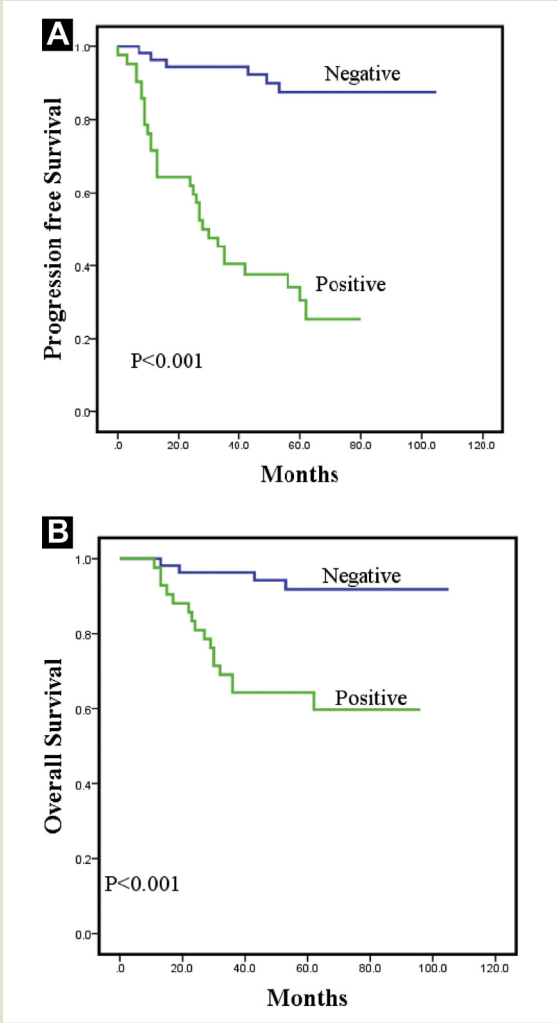

Abbreviations: PFS = progression-free survival; OS = overall survival.

Gal-1−targeted immunotherapy[27-30] and to monitor their response to treatment.

A previous meta-analysis identified high Gal-1 expression as a predictor of poor prognosis in patients with cancer.[31] Only 2 studies that were included in the review investigated the prognostic significance of Gal-1 expression in lung cancer.[18,19] In one study of radically operated patients with stage II NSCLC, Gal-1−positive patients had poor prognosis on univariate but not multivariate analysis.[18] In another study of patients with stage I-III NSCLC, tumor Gal-1 expression was associated with poor clinical outcomes on multivariate analysis.[19] The present study identified tumor Gal-1 expression as a significant independent prognostic factor for PFS but not OS. The contrasting findings of the present study and those of previous studies regarding the prognostic significance of Gal-1 in NSCLC may be due to differences in the study design, including the lung adenocarcinoma disease stage, the inclusion of tumor and/or tumor stromal cells in the immunohistochemical analyses, and

Table 3 Univariate and Multivariate Analyses of Prognostic Factors for Progression-Free Survival and Overall Survival

	Progression-Free Survival				Overall Survival			
	Univariate Analysis		Multivariate Analysis		Univariate Analysis		Multivariate Analysis	
Factor	OR (95% CI)	*P*	OR (95% CI)	*P*	OR (95% CI)	*P*	OR (95% CI)	*P*
Age								
≥65 years/< 65 years	1.000 (0.965-1.037)	.999			1.021 (0.974-1.071)	.393		
Sex								
Male/female	0.544 (0.279-1.058)	.073			0.359 (0.143-0.901)	.029		
Smoking History								
Smoker/never smoker	0.963 (0.472-1.968)	.918			1.432 (0.585-3.506)	.431		
Tumor Differentiation								
Poor-moderate/well	4.583 (1.896-11.079)	.001			2.367 (0.860-6.517)	.095		
Tumor Size								
<3 cm/≥ 3 cm	1.198 (0.911-1.574)	.196			1.096 (0.748-1.606)	.639		
Lymph Node Metastasis								
$N_0/N_{\geq 1}$	5.766 (2.942-11.300)	<.0001			7.173 (2.854-18.028)	<.0001		
TNM Stage								
I-II/III-IV	6.571 (3.331-12.962)	<.0001	3.270 (1.602-6.674)	.001	8.895 (3.610-21.921)	<.0001	6.279 (2.427-16.244)	<.0001
Gal-1 Expression								
Positive/negative	9.945 (4.099-24.128)	<.0001	7.087 (2.798-17.948)	<.0001	6.250 (2.086-18.730)	.001		
SUV_{max}								
High/low	1.135 (1.083-1.189)	<.0001			1.124 (1.057-1.196)	<.0001	1.087 (1.011-1.169)	.024
MTV								
High/low	1.026 (1.012-1.039)	<.0001			1.022 (1.004-1.041)	.018		
TLG								
High/low	1.005 (1.003-1.008)	<.0001			1.005 (1.001-1.008)	.006		

Abbreviations: CI = confidence interval; Gal-1 = galectin-1; MTV = metabolic tumor volume; OR = odds ratio; SUV_{max} = standardized maximum uptake value; TLG = total lesion glycolysis; TNM = tumor, node, metastasis classification system.

the length of the follow-up period. These factors may confound the results, as tumor stage is an important prognostic indicator, Gal-1 expression in tumor stroma was not of prognostic significance for OS, and the length of follow-up period must be long enough to determine the prognostic significance of tumor Gal-1 status for OS.[32] Despite this, findings from the present study as well as previous studies indicate that tumor Gal-1 expression is a potential novel biomarker for predicting NSCLC recurrence after surgery and identifying patients who would benefit from appropriate intervention.

GLUT-1 and HK-II are key rate-limiting enzymes for glycolysis. As a glucose analog, ^{18}F-FDG is transported into tumor cells by GLUT-1 and trapped intracellularly. The present study showed significant positive correlations between GLUT-1 and HK-II immunohistochemistry scores and SUV_{max} as well as the GLUT-1, HK-II, and Gal-1 immunohistochemistry scores. Accordingly, in previous studies of colorectal cancer tissue, Gal-1 expression was shown to be highly correlated with GLUT-1 expression.[13] Park and Kim[24] reported that Toll-like receptor 4 (TLR4) activation increased Gal-1 expression, triggered the activation of glycolysis-related enzymes and promoted lactate production. Furthermore, inhibition of Gal-1 attenuated the activity of glycolysis-related enzymes, including HK-II, phosphofructokinase (PFKP), pyruvate kinase M2 (PKM2), and lactate dehydrogenase A (LDHA). A TLR agonist induced a metabolic transition from oxidative phosphorylation to aerobic glycolysis, which was mediated by the PI3K/Akt-mediated AMP-AMPK signaling pathway.[33] Taken together, these data indicate that Gal-1 is involved in the regulation of glycolysis in tumors.

In this study, advanced tumor stage and Gal-1 expression were independent prognostic indicators of poor PFS, while advanced tumor stage and SUV_{max} were independent prognostic indicators of poor OS. In contrast, previous research reported that MTV and TLG more accurately reflect the metabolic status of a malignancy and are better prognostic markers than SUV_{max} in lung cancer.[34,35] The small sample size, single center, and retrospective nature of our study may explain this difference.

This study had several limitations. First, it was performed at a single center with a small sample size, and the retrospective study design had unavoidable selection bias. A multicenter prospective study with a larger sample size is warranted. Second, follow-up time was relatively short; in the future, our research will focus on the prognostic significance of tumor Gal-1 status for OS. Third, although we confirmed the associations between FDG uptake and Gal-1 protein expression, the underlying mechanisms remain unclear. We plan to conduct in vitro experiments to investigate the mechanisms by which Gal-1 affects glycolysis. Fourth, in our study, SUV_{max} was the only independent predictor of tumor Gal-1 expression. SUV_{max} is the most commonly used parameter in clinical practice because of its simplicity. However, many factors influence SUV_{max}, including patient-level variables (eg, body weight, stature, serum glucose level), imaging procedures (eg, leakage of intravenous injection), the PET/CT scanner (model, scintillation crystal array and photo detector, reconstruction and image processing), and clinical variables, especially tumor size; in lesions < 3.0 cm, SUV_{max} is influenced by spatial resolution and partial volume effects. To ensure reproducibility of our technique, the Biograph True Point PET/CT scanner (Siemens Medical Systems) in our department meets the National Electrical Manufacturers Association NU 2−2007 performance standard, tumor imaging is performed according to the European Association of Nuclear Medicine procedure guidelines, and a quality control/quality assurance procedure is conducted to maintain the accuracy and precision of quantitation.

Conclusion

^{18}F-FDG uptake was positively correlated with tumor Gal-1 expression in patients with lung adenocarcinoma. Tumor Gal-1 expression and SUV_{max} were significant predictors of PFS and OS, respectively. These data suggest that ^{18}F-FDG PET/CT has potential as a noninvasive imaging modality to assess tumor Gal-1 status and prognosis in lung adenocarcinoma.

Clinical Practice Points

- There remains an unmet clinical need to identify new immune biomarkers and therapeutic targets in NSCLC. Noninvasive imaging modalities could be beneficial.
- PET/CT parameters positively correlated with tumor Gal-1 expression in patients with lung adenocarcinoma.
- SUV_{max} was the only independent predictor of tumor Gal-1 expression. On multivariate analysis, tumor Gal-1 expression and SUV_{max} were independent predictors of prognosis.
- PET/CT can predict tumor Gal-1 expression and may be used to select patients who will gain the most benefit from Gal-1−targeted immunotherapy and to monitor their response to treatment.

Acknowledgments

Supported in part by the National Natural Science Foundation of China (grant 81771868). The authors thank Medjaden Bioscience Limited for editorial work.

Disclosure

The authors have stated that they have no conflict of interest.

References

1. Siegel RL, Miller KD, Jemal A. Cancer statistics, 2018. *CA Cancer J Clin* 2018; 68: 7-30.
2. Little AG, Gay EG, Gaspar LE, et al. National survey of non−small cell lung cancer in the United States: epidemiology, pathology and patterns of care. *Lung Cancer* 2007; 57:253-60.
3. Didkowska J, Wojciechowska U, Manczuk M, et al. Lung cancer epidemiology: contemporary and future challenges worldwide. *Ann Transl Med* 2016; 4:150.
4. Raju S, Joseph R, Sehgal S. Review of checkpoint immunotherapy for the management of non−small cell lung cancer. *Immunotargets Ther* 2018; 7:63-75.
5. Sharma P, Allison JP. Immune checkpoint targeting in cancer therapy: toward combination strategies with curative potential. *Cell* 2015; 161:205-14.
6. Mendez-Huergo SP, Blidner AG, Rabinovich GA. Galectins: emerging regulatory checkpoints linking tumor immunity and angiogenesis. *Curr Opin Immunol* 2017; 45:8-15.
7. Barondes SH, Castronovo V, Cooper DN, et al. Galectins: a family of animal beta-galactoside−binding lectins. *Cell* 1994; 76:597-8.
8. Chung LY, Tang SJ, Sun GH, et al. Galectin-1 promotes lung cancer progression and chemoresistance by upregulating p38 MAPK, ERK, and cyclooxygenase-2. *Clin Cancer Res* 2012; 18:4037-47.
9. Hsu YL, Wu CY, Hung JY, et al. Galectin-1 promotes lung cancer tumor metastasis by potentiating integrin α6β4 and Notch1/Jagged2 signaling pathway. *Carcinogenesis* 2013; 34:1370-81.
10. White NM, Masui O, Newsted D, et al. Galectin-1 has potential prognostic significance and is implicated in clear cell renal cell carcinoma progression through the HIF/mTOR signaling axis. *Br J Cancer* 2017; 116:e3.

11. Chen L, Yao Y, Sun L, et al. Galectin-1 promotes tumor progression via NF-kB signaling pathway in epithelial ovarian cancer. *J Cancer* 2017; 8:3733-41.
12. Rubinstein N, Alvarez M, Zwirner NW, et al. Targeted inhibition of galectin-1 gene expression in tumor cells results in heightened T cell−mediated rejection: a potential mechanism of tumor-immune privilege. *Cancer Cell* 2004; 5:241-51.
13. Zhao XY, Chen TT, Xia L, et al. Hypoxia inducible factor-1 mediates expression of galectin-1: the potential role in migration/invasion of colorectal cancer cells. *Carcinogenesis* 2010; 31:1367-75.
14. Banh A, Zhang J, Cao H, et al. Tumor galectin-1 mediates tumor growth and metastasis through regulation of T-cell apoptosis. *Cancer Res* 2011; 71:4423-31.
15. Hsu YL, Hung JY, Chiang SY, et al. Lung cancer−derived galectin-1 contributes to cancer associated fibroblast-mediated cancer progression and immune suppression through TDO2/kynurenine axis. *Oncotarget* 2016; 7:27584-98.
16. Andersen MN, Ludvigsen M, Abildgaard N, et al. Serum galectin-1 in patients with multiple myeloma: associations with survival, angiogenesis, and biomarkers of macrophage activation. *Onco Targets Ther* 2017; 10:1977-82.
17. Bacigalupo ML, Carabias P, Troncoso MF. Contribution of galectin-1, a glycan-binding protein, to gastrointestinal tumor progression. *World J Gastroenterol* 2017; 23:5266-81.
18. Szoke T, Kayser K, Trojan I, et al. The role of microvascularization and growth/adhesion-regulatory lectins in the prognosis of non−small cell lung cancer in stage II. *Eur J Cardiothorac Surg* 2007; 31:783-7.
19. Carlini MJ, Roitman P, Nunez M, et al. Clinical relevance of galectin-1 expression in non−small cell lung cancer patients. *Lung Cancer* 2014; 84:73-8.
20. Punt S, Thijssen VL, Vrolijk J, et al. Galectin-1, -3 and -9 expression and clinical significance in squamous cervical cancer. *PLoS One* 2015; 10:e0129119.
21. Chou SY, Yen SL, Huang CC, et al. Galectin-1 is a poor prognostic factor in patients with glioblastoma multiforme after radiotherapy. *BMC Cancer* 2018; 18:105.
22. Budak E, Cok G, Akgun A. The contribution of fluorine ^{18}F-FDG PET/CT to lung cancer diagnosis, staging and treatment planning. *Mol Imaging Radionucl Ther* 2018; 27:73-80.
23. Lee MY, Han HJ. Galectin-1 upregulates glucose transporter-1 expression level via protein kinase C, phosphoinositol-3 kinase, and mammalian target of rapamycin pathways in mouse embryonic stem cells. *Int J Biochem Cell Biol* 2008; 40:2421-30.
24. Park GB, Kim D. TLR4-mediated galectin-1 production triggers epithelial mesenchymal transition in colon cancer cells through ADAM10 and ADAM17-associated lactate production. *Mol Cell Biochem* 2017; 425:191-202.
25. Edge SB, Byrd DR, Compton CC, Fritz AG, Greene FL, Trotti A, eds. *AJCC Cancer Staging Manual*. 7th ed. New York, NY: Springer; 2010.
26. Schulz H, Schmoeckel E, Kuhn C, et al. Galectins-1, -3 and -7 are prognostic markers for survival of ovarian cancer patients. *Int J Mol Sci* 2017; 18:1230-41.
27. Ito K, Scott SA, Cutler S, et al. Thiodigalactoside inhibits murine cancers by concurrently blocking effects of galectin-1 on immune dysregulation, angiogenesis and protection against oxidative stress. *Angiogenesis* 2011; 14:293-307.
28. Croci DO, Salatino M, Rubinstein N, et al. Disrupting galectin-1 interactions with *N*-glycans suppresses hypoxia-driven angiogenesis and tumorigenesis in Kaposi's sarcoma. *J Exp Med* 2012; 209:1985-2000.
29. Astorgues-Xerri L, Riveiro ME, Tijeras-Raballand A, et al. OTX008, a selective small-molecule inhibitor of galectin-1, downregulates cancer cell proliferation, invasion and tumour angiogenesis. *Eur J Cancer* 2014; 50:2463-77.
30. Koonce NA, Griffin RJ, Dings RPM. Galectin-1 inhibitor OTX008 induces tumor vessel normalization and tumor growth inhibition in human head and neck squamous cell carcinoma model. *Int J Mol Sci* 2017; 18:E2671.
31. Wu R, Wu T, Wang K, et al. Prognostic significance of galectin-1 expression in patients with cancer: a meta-analysis. *Cancer Cell Int* 2018; 18:108.
32. Wu H, Chen P, Liao R, et al. Overexpresssion of galectin-1 is associated with poor prognosis in human hepatocellular carcinoma following resection. *J Gastroenterol Hepatol* 2012; 27:1312-9.
33. Krawczyk CM, Holowka T, Sun J, et al. Toll-like receptor−induced changes in glycolytic metabolism regulate dendritic cell activation. *Blood* 2010; 115:4742-9.
34. Takahashi N, Yamamoto T, Matsushita H, et al. Metabolic tumor volume on FDG-PET/CT is a possible prognostic factor for stage I lung cancer patients treated with stereotactic body radiation therapy: a retrospective clinical study. *J Radiat Res* 2016; 57:655-61.
35. Sharma A, Mohan A, Bhalla AS, et al. Role of various metabolic parameters derived from baseline ^{18}F-FDG PET/CT as prognostic markers in non−small cell lung cancer patients undergoing platinum-based chemotherapy. *Clin Nucl Med* 2018; 43:e8-17.